

12

AD

AD-E401 035

TECHNICAL REPORT ARLCD-TR-83030

A METHOD TO EVALUATE THE BURNING BEHAVIOR
OF SECONDARY EXPLOSIVES - COMPOSITION B

RODOLF W. VELICKY

JUNE 1983

DTIC
ELECTED
JUN 16 1983
S D
B



US ARMY ARMAMENT RESEARCH AND DEVELOPMENT COMMAND
LARGE CALIBER
WEAPON SYSTEMS LABORATORY
DOVER, NEW JERSEY

APPROVED FOR PUBLIC RELEASE: DISTRIBUTION UNLIMITED.

DTIC FILE COPY

83 06 14 042

AD A 130 004

(12)

AD

AD-E401 035

TECHNICAL REPORT ARLCD-TR-83030

A METHOD TO EVALUATE THE BURNING BEHAVIOR
OF SECONDARY EXPLOSIVES - COMPOSITION B

RODOLF W. VELICKY

JUNE 1983

DTIC
ELECTE
S JUN 16 1983 D
B



US ARMY ARMAMENT RESEARCH AND DEVELOPMENT COMMAND
LARGE CALIBER
WEAPON SYSTEMS LABORATORY
DOVER, NEW JERSEY

APPROVED FOR PUBLIC RELEASE; DISTRIBUTION UNLIMITED.

DTIC FILE COPY

83 06 14 04

The views, opinions, and/or findings contained in this report are those of the author(s) and should not be construed as an official Department of the Army position, policy, or decision, unless so designated by other documentation.

Destroy this report when no longer needed. Do not return to the originator.

UNCLASSIFIED

SECURITY CLASSIFICATION OF THIS PAGE (When Data Entered)

REPORT DOCUMENTATION PAGE		READ INSTRUCTIONS BEFORE COMPLETING FORM
1. REPORT NUMBER Technical Report ARLCD-TR-83030	2. GOVT ACCESSION NO. A21160 C04	3. RECIPIENT'S CATALOG NUMBER
4. TITLE (and Subtitle) A METHOD TO EVALUATE THE BURNING BEHAVIOR OF SECONDARY EXPLOSIVES - COMPOSITION B		5. TYPE OF REPORT & PERIOD COVERED
		6. PERFORMING ORG. REPORT NUMBER
7. AUTHOR(s) Rodolf W. Velicky		8. CONTRACT OR GRANT NUMBER(s)
9. PERFORMING ORGANIZATION NAME AND ADDRESS ARRADCOM, LCWSL Energetic Materials Div (DRDAR-LCE) Dover, NJ 07801		10. PROGRAM ELEMENT, PROJECT, TASK AREA & WORK UNIT NUMBERS Proj 1L162603AH18
11. CONTROLLING OFFICE NAME AND ADDRESS ARRADCOM, TSD STINFO Div (DRDAR-TSS) Dover, NJ 07801		12. REPORT DATE June 1983
14. MONITORING AGENCY NAME & ADDRESS (if different from Controlling Office)		13. NUMBER OF PAGES 38
		15. SECURITY CLASS. (of this report) Unclassified
		15a. DECLASSIFICATION/DOWNGRADING SCHEDULE
16. DISTRIBUTION STATEMENT (of this Report) Approved for public release; distribution unlimited.		
17. DISTRIBUTION STATEMENT (of the abstract entered in Block 20, if different from Report)		
18. SUPPLEMENTARY NOTES		
19. KEY WORDS (Continue on reverse side if necessary and identify by block number) Comp B Explosive Combustion Burning Deflagration Closed bomb In-bore prematures Hazard		
20. ABSTRACT (Continue on reverse side if necessary and identify by block number) It is demonstrated in this work that the closed bomb can be used to detect changes in the burning properties of Composition B that are caused by small modifications to its composition. It is shown that, upon ignition, Composition B first burns on the surface as do standard gun propellants. It then undergoes a transition during which the initial physical configuration breaks up into fragments. This produces an increased surface area whose creation rate is determined by the particular additive coated on the Cyclotrimethylenetrinitramine (RDX) particles. There are additives, such as estane, which can slow the		

UNCLASSIFIED

SECURITY CLASSIFICATION OF THIS PAGE (When Data Enclosed)

20. ABSTRACT (cont)

surface area creation rate more effectively than does the standard wax used in Composition B.

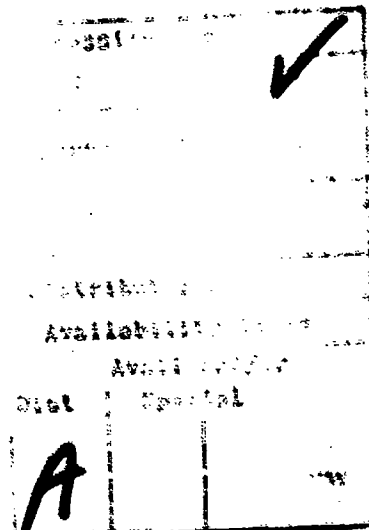
The closed bomb can provide the explosive formulator with a powerful laboratory tool which will allow him to monitor the results of his efforts to reduce the deflagration hazards of explosives. Also, with additional work, this tool can help unravel the deflagration mechanisms associated with energetic materials.

UNCLASSIFIED

SECURITY CLASSIFICATION OF THIS PAGE (When Data Enclosed)

CONTENTS

	Page
Introduction	1
Experimental	1
Procedure	2
Results and Discussion	2
Pressure Versus Time Measurements	2
Linear Burning Rate Calculations	3
Quickness Measurements	3
Comp B Interrupted Burning Test	4
Relationship of Additives to Formation of the Complex	4
Effect of Additives on Composition B Burning	5
Intrinsic Burn Rate of RDX Particle from Closed Bomb Measurements	5
Conclusions	6
Recommendations	7
References	9
Distribution List	27



TABLES

	Page
1 Composition B, linear burning rate calculation	11
2 Composition BW, linear burning rate calculation	12
3 Composition B4, linear burning rate calculation	13
4 Closed bomb burning rate of RDX - various particle sizes	14

FIGURES

1 Composition B, solid cylinder, 3/8 single perf, and crushed	15
2 Composition BW, solid cylinder and 3/8 single perf (estane on RDX)	16
3 Composition B4, solid cylinder and single perf (without additives)	17
4 Composition B, standard type with wax, test #1	18
5 Composition B, standard type with wax, test #2	19
6 Composition B, standard type with wax, test #3	20
7 Composition BW, estane precoated on the RDX particle	21
8 Composition B4, without additives	22
9 Composition A3, pressed to a density of 1.640 g/cm ³	23
10 Comparison of additives in variations of Composition B	24
11 Closed bomb burning rates of the RDX particle	25

INTRODUCTION

Explosive fills for munitions are designed to be difficult to accidentally detonate. A complicated, though well understood, explosive train technology is required to intentionally stimulate these materials to a detonation. Almost all hazards associated with military explosives begin with burning. A modest thermal initiation (hot spot) can quickly develop into a catastrophe. Typical problem areas are in large caliber weapon in-bore prematures and munitions that are damaged by fragment attack.

Attempts have been made to improve some military explosives in order to reduce this deflagration hazard. These programs failed because the mechanism controlling the reaction rates is not well understood. In addition, there was no laboratory test which could evaluate an improvement.

It is the purpose of this report to show that an old, well-established, technique can be used to expose the factors controlling the burning mechanism of explosives. It will be demonstrated that slight modifications of an explosive composition can significantly slow the reaction rate of these materials. This method can provide the explosive formulator with a testing procedure that will permit him to monitor the results of his efforts to reduce deflagration hazards.

EXPERIMENTAL

The tool used in this study is the closed bomb. The standard closed bomb is a heavy-walled steel container with an internal volume of about 200 cm³. It contains a closure with an insulated firing electrode, an exhaust valve, and a piezo pressure transducer. Gases that are generated by burning energetic materials can be contained within the vessel to a pressure of about 690 MPa (100,000 psi). The pressure versus time data developed by these reactions are electronically recorded and stored for computer calculations.

This tool is the work horse of the propellant industry. It is routinely used to evaluate surface burning propellant compositions. This is done according to well-established procedures described in references 1 through 11.

Explosives are not, generally, surface burning materials. The physical configuration usually breaks up to produce a new surface area at some point during the burning. This does not invalidate the procedure. These materials are burning on the new surface with the intrinsic burning rate of the composition. An effort is needed to determine the rate at which the new surface area is being created, the dimensions of the new geometry, and the intrinsic burning rate of the composition.

PROCEDURE

Much of this work was reported in reference 12. This is another look at those data with computer tools which were not available at that time. Additional work which was subsequently performed is also included. Composition (Comp) B is the explosive vehicle for this study. The method, however, is applicable to other energetic compositions.

Precise cylindrical geometries were machined from cast Comp B (1% wax), Comp BW (1% estane), Comp B4 (no additives), and Comp A3 (RDX/WAX, 91/9). They were machined to provide two significantly different surface areas with respect to the volume fraction burned for each sample. They were 2.54 cm diameter cylinders. One was solid and the other, a single perforated grain, contained a 0.953 cm hole in the center. The lengths were adjusted to provide a constant mass and were approximately 5 cm long. A crushed form of Comp B was also tested. The intent for these samples was to test for surface burning according to the "propellant linear burning rate theory".

Two forms of Comp B with estane were tested. In one case, the estane was precoated on the RDX particle, and, in the other, it was mixed into the hot TNT melt. These samples in relation to Comp B with and without the standard wax additive were used to ascertain the role performed by additives in the RDX/TNT mixture. Each test was provided with massive thermal ignition with 5 grams of class 7 black powder. This was done to insure simultaneous ignition of the entire surface area.

RDX is a major constituent of Comp B. Information on its intrinsic burning rate would be important for understanding the burning mechanism of Comp B. Therefore, an attempt was made to develop a technique to determine the linear burning rate as a function of pressure for the RDX particle.

RESULTS AND DISCUSSION

Pressure Versus Time Measurements

The results reported in reference 12 showed that Comp B and variations thereof exhibited a transition from slow to fast burning. This transition occurred at a pressure of 60 to 130 MPa. Figures 1 through 3 illustrate this transition for Comp B (wax), Comp BW (estane), and Comp B4 (no additives). These curves are overlapped as the maximum pressure is approached. Zero time refers to the start of data recording.

Each figure compares the pressure developed with respect to time for the burning of the two geometries (solid cylinder and 1/8 in. single pellet). Figure 1 also includes the burning of crushed Comp B. This was material from the same casting which was mechanically crushed into an aggregate of fine powder and some small chunks. Initially, the burning of each sample is influenced by the original geometry. Then, all the variations of Comp B show a transition to a common burning region. Figure 1 shows that the mechanically deconsolidated

Comp B also shares this common burning region with the solid castings. This strongly suggests that, at the transition, the physical structure of Comp B is breaking up, creating new (increased) surface area.

Linear Burning Rate Calculations

A linear burning rate analysis, based on the "propellant linear burning rate theory", was performed on each side of the transition for each sample. This analysis requires that burning progresses only on the surface of the sample (cigarette style). When all the requirements are met, the procedure will measure the true burning rate. The results for a particular composition would be the same for any known geometry.

The results of these calculations are shown in tables 1 through 3. In the after-transition region, it is observed that the burning rates derived for the two geometries do not agree for any of the Comp B variations. This shows that the physical structure had changed. Burning in this region is progressing on a new surface area that is not represented by a surface area regression that is normal to the original surface. This could be interpreted as a breakup of the physical structure of Comp B. A breakup would increase the surface area, which in turn would dramatically increase the burning velocity.

In the pre-transition region, Comp B and Comp BW (tables 1 and 2) demonstrate a good example of propellant-type surface burning. The burning rate agreement derived for the two geometries is excellent for Comp BW to a pressure of 70 MPa. Regular Comp B shows a slight divergence as this pressure is approached and Comp B4 (no additives) shows a wide divergence with poor reproducibility (table 3). This behavior could indicate that burning is beginning to penetrate into the sample body as a prelude to the breaking up of the physical structure.

Quickness Measurements

The differentiation of the pressure versus time curve (dp/dt vs pressure) is used to calculate the linear burning rate. When unusual burning behavior is encountered, as is the case with Comp B, an examination of this quickness curve can provide a means of understanding the process. Since these curves do not directly evaluate fundamental properties, they must be used on a comparison basis. Introducing controlled variations, such as surface area, particle size, concentration, and composition (additive), will produce test results which can be evaluated on a cause and effect basis.

Figures 4 through 9 utilize the quickness curve to compare the burning behavior of samples which have very different initial surface areas (solid cylinder and 3/8 10 single perf). This was done for the three variations of Comp B and for Comp AJ. Composition AJ is RDX/WAX (91/9) which had been pressed to a density of 1.640 g/cm³. Since the mass and composition of these samples are the same, the dp/dt (quickness) compares the surface areas burning. The slope of each curve is an indication of the rate at which that surface area is being created.

Comp B demonstrates the surface burning phase, prior to transition, with the normal divergence in quickness associated with a variation of the initial surface area (figures 4, 5, and 6). A very interesting observation, however, is made in the after-transition region. The sample which begins burning with the largest surface area (3/8 ID single perf) creates a lesser total surface area with respect to the solid cylinder. One possible explanation of this is that the magnitude of the initial surface area of the sample somehow ties up a volume of material proportional to the surface area and this material does not participate in the breakup that follows the transition.

Comp B Interrupted Burning Test

Supporting evidence for this idea is provided by work performed at Los Alamos National Laboratory (LANL) (ref 13). They performed an interrupted burning test on Comp B. A slab of this explosive was ignited, partially burned, and then quenched. This was done at atmospheric pressure. The quenched explosive was sectioned, polished, and microscopically examined. This showed that, to a considerable depth below the extinguished surface, there was a zone of complete RDX depletion. Thereafter, the RDX particles became visible and quickly increased to the normal size. This zone of RDX depletion implies, for want of a better term, the formation of a complex. A complex of this type is the concept needed to explain the reversal of surface area creation shown in Comp B quickness curves. A complex, formed under the burning surface during the surface burning phase, would tie up a volume of material proportional to the surface area. If the complex were not involved in the breakup, the 3/8 ID single perf grain, at transition, would have a lesser volume of material available for breaking up into a proportionally lesser total surface area than would the solid cylinder.

In addition, the existence of a complex helps to resolve another dilemma. TNT is the binder for RDX in the explosive Comp B. References 12 and 14 show that the physical structure of TNT breaks up at the very beginning of combustion. Until the concept of the formation of a complex was introduced, it was difficult to understand why the 40% TNT binder did not break up to provide a new burning surface when burned in union with RDX, as it did when burned alone.

Relationship of Additives to Formation of the Complex

Comp BW (fig. 7), like Comp B, also demonstrates the reversal of surface area creation with respect to the initial surface area of the sample. In figures 8 and 9, it is observed that Comp B4 (no additives) and Comp A3 (no TNT) do not burn in this manner. The sample, which breaks up first (3/8 ID single perf) creates the greatest surface area. This is reasonable and expected, if there is no complex near the surface, restricting a portion of the material from participating in the breakup. It follows that an additive is required in the presence of both RDX and TNT in order to form the complex.

Effect of Additive on Comp B Burning

In figure 10, the quickness curve is used to compare the burning of several Comp B variations. The variable is the 1% additive. A quick glance shows that the presence of an additive (wax or estane) is needed to establish the surface burning phase of combustion. The estane comparison shows that the location of the additive is extremely important. When estane was pre-coated on the RDX particle, as opposed to being mixed into the TNT, it slowed the burning of the explosive more effectively. It did this by slightly extending the pre-transition surface burning phase. More important, however, a comparison of the slopes indicates that the rate of fragment creation is slowed because the additive is coated on the RDX particles. This suggests that, using the closed bomb as an evaluating tool, a search should be undertaken for the ideal additive (coating).

Observations made, concerning regular Comp B, suggest that the manufacturing process automatically coats the RDX particle with wax. The work reported in reference 14 shows that wax does not change the burning characteristics of TNT. It also pointed out that wax is virtually unmixable with TNT. However, when crystalline RDX is added to the hot TNT/wax melt, the wax is easily drawn into the mixture. The only possible place for it to go is on the surface of the RDX particle.

Logically, it follows that an inert coating on the RDX particle must function as an inhibitor. The inhibitor must delay, even if only infinitesimally, the initiation of each particle. The total effect of these delays would be to slow the rate of surface area reaction. When the search for the ideal additive is made, materials with good insulating and thermal stability properties should be considered first.

Intrinsic Burn Rate of RDX Particle from Closed Bomb Measurements

The closed bomb can do more than function as a day-to-day working tool. It can help unravel the burning mechanism of explosives such as Comp B. The thermodynamics and physics of the transition zone must be very complicated, but the interface of this zone must accelerate as a function of pressure into the body of the unreacted solid. It must leave behind fragments with a gradient in both size (related to fraction burned) and particle density (space between particles). These particles or fragments must burn individually on their surfaces according to surface burning linear regression laws. It is not known how the RDX and TNT interact with each other during this phase of burning, but knowing the intrinsic burning rate of the constituents would be helpful toward unraveling the mystery.

Therefore, an attempt was made to develop a method to determine the burning rate of RDX as a function of pressure from closed bomb calculations. The assumption is made that the RDX particle burns on its surface, and a linear regression analysis of the correct geometry will develop the same burning rates with respect to pressure for RDX with different particle sizes.

Class 7 black powder, the standard igniter used in closed bomb work, burns slower than the RDX that it is intended to ignite. Reasonable success was

obtained by using Hivelite powder, a very high burning-rate propellant, as an igniter. An approach to the simultaneous ignition of the entire surface area is extremely important to this analysis. In the work discussed here, 25% to 30% of the RDX had been consumed before total surface area ignition was obtained. This can be improved in the future by dividing the charge and igniting many small packets. This may also have the advantage of cancelling out the development of pressure waves.

A straight line log-log burning rate curve is developed when a material burns on the surface and the correct geometrical shape is used in the calculations. This was the result when a sphere was assumed for the configuration of RDX (figure 11, table 4). Apparently, the particle melts and cohesive forces pull it into the configuration of a sphere, which then burns on the surface. The particle diameter used in the calculations were crudely estimated from an average of a sieve size cut. They contain a significant error which could change the coefficient in the burning rate equation. In the future, the particle diameter will be based on its density and average mass.

When applied to RDX, the exponent, n , in the burning rate equation

$$r = aP^n$$

where

r = rate, cm/s

P = pressure, MPa

is about 0.7 to 0.8. This is a reasonable value for an energetic material. The coefficient, a , is about 1.0. This value is probably in gross error; the intention, however, is to point out an approach for determining the intrinsic burning rate of RDX that may have potential.

CONCLUSIONS

The closed bomb can be used as a working tool to observe the burning behavior of explosives. It can expose the factors controlling the burning even if the fundamentals of the mechanism are not completely understood. In an explosive like Comp B, it has been demonstrated that a modification to its burning behavior can be observed. The additive estane (coated on the RDX particle) slows the burning more effectively than wax. There must be many other materials that can slow the burning more, thus making a safer Comp B. The closed bomb, a simple laboratory tool, can be used to select the additive which would do this.

In addition, there are observations, drawn from the closed bomb, that can provide a guide to the explosive formulator in the search for an improved Comp B.

1. Comp B undergoes a transition from a region where the material burns on its surface to where the composition breaks up and burns on the newly-created surface of its fragmented parts.
2. During the initial surface burning phase, a complex is formed at a significant depth below the surface. This blend of RDX and TNT does not participate in the breakup phase of burning.
3. The formation of the complex requires the presence of an additive (wax or estane).
4. Additives can change the rate at which new surface area is being created during the breakup phase of burning. Some additives do this more effectively than others.
5. Additives modify the burning of Comp B because they are coated on the RDX particle.
6. Additives appear to act as inhibitors which infinitesimally delay the initiation of each RDX particle.
7. Particles of RDX melt and form spheres which burn on the surface when they are burned alone. It is highly probable that they do so when released from the Comp B solid during the breakup phase of burning.

RECOMMENDATIONS

The work, as described in this report, was a learning experience. Much was learned about the use of the equipment, the interpretation of the data, and the burning behavior of Comp B. Insight into the combustion process of Comp B was developed, but much of it is interpretive and based on inference. The work needs to be expanded and placed on a solid foundation. A period of acquiring data, with scrupulous attention to detail, is needed.

The objective of this work should be to separate and measure the rate of surface area creation from the intrinsic burning rate of the fragmented parts. These fundamental properties could then be combined in suitable equations to predict explosive-burning in situations that might occur in in-bore prematures and munitions damaged by fragment attack.

An accurate measurement of the intrinsic burning rate of TNT and the RDX particle is needed in relation to closed bomb measurements on specially-made Comp B samples. These samples should incorporate variations in all parameters which affect its burning behavior (i.e. RDX particle size, its concentration, substitute additives, additive concentration, etc.). Utilizing the intrinsic burning rate of the constituents in combination with various possibilities, it may be possible to develop equations which describe the burning behavior of Comp B.

REFERENCES

1. W.E. Jordan, "Closed Bomb Method of Powder Testing," E.I. duPont Memorandum Report No. 24, Explosives Department, Burnside Laboratory, 26 February 1941.
2. S.J. Jacobs and W.B. Buck, "Closed Bomb Burning of High Explosives and Propellants," OSRD Report No. 6329, 22 January 1946.
3. C.M. Dickey, "Determination of Burning Characteristics of Propellants," E.I. duPont Memorandum Report No. 31, 8 March 1943.
4. A.T. Wilson, "Improved Propellants for Small Arms," Final Report, National Fireworks Co., West Hanover, MS, 15 March 1950.
5. D.S. Davis, "Empirical Equations and Nomography," First Edition, McGraw-Hill Book Co., Inc., New York and London, 1943.
6. J.O. Hirschfelder and J. Sherman, "Simple Calculations of Thermochemical Properties for Use in Ballistics," OSRD Report No. 1300, 5 March 1943.
7. J.O. Hirschfelder, R.B. Kershner, and C.F. Curtis, "Interior Ballistics I," OSRD Report No. 1236, 4 February 1943.
8. E.H. Julier, "Form Functions for Use in Interior Ballistics and Closed Chamber Calculations," Memorandum Report No. 3, Naval Powder Factory, Indianhead, MD, 13 February 1951.
9. L.G. Bonner, "Determination of the Linear Burning Rates of Propellants from Pressure Measurements in the Closed Chamber," OSRD Report No. 4382, 30 November 1944.
10. J.P. Vinti, "Powder Gas Data for Typical Powders," Memorandum Report No. 214, Ballistic Research Laboratories, Aberdeen, MD, 15 September 1943.
11. A. Pallingston and M. Weinstein, "Method of Calculation of Interior Ballistic Properties of Propellants from Closed Bomb Data," Picatinny Arsenal Technical Report 2005, Picatinny Arsenal, Dover, NJ, June 1954.
12. R.W. Velicky and J. Hershkowitz, "Anomalous Burning Rate Characteristics of Composition B and TNT," Seventh Symposium (International) on Detonation, 1981.
13. J. Hershkowitz, Consultant, Private Communication, 305 Passaic Avenue, West Caldwell, NJ, 07006.
14. R.W. Velicky, "The Burning Behavior of TNT in the Closed Bomb," Technical Report ARLCD-TR-83015, ARRADCOM, Dover, NJ, March 1983.

Table 1. Composition B, linear burning rate calculation

Pre-transition region			After-transition region		
Pressure ^a MPa	Burning rate, cm/s		Pressure ^b MPa	Burning rate, cm/s	
	Solid	Perf		Solid	Perf
13.79	1.0±0.5	1.1±0.6	179.3	280±25	76±21
20.68	1.7±0.6	1.8±0.8	193.1	308±26	81±19
27.58	2.6±0.6	2.6±1.0	206.8	337±26	85±18
34.47	3.5±0.5	3.5±1.0	220.6	366±26	89±16
41.37	4.6±0.4	4.4±1.0	234.4	396±27	94±15
48.26	5.8±0.3	5.3±1.0	248.2	426±27	98±13
55.16	7.1±0.6	6.3±0.9	262.0	457±27	102±12
62.05	8.5±1.0	7.4±0.8	275.8	488±27	106±11
68.95	10.0±1.6	8.5±0.7	289.6	520±27	111±10

^aPressure (MPa) equivalent to pressure (psi) 2K to 10K step 1K.

^bPressure (MPa) equivalent to pressure (psi) 26K to 42K step 2K.

Table 2. Composition BW, linear burning rate calculation

Pre-transition region			After-transition region		
Pressure ^a MPa	Burning rate, cm/s		Pressure ^b MPa	Burning rate, cm/s	
	Solid	Perf		Solid	Perf
13.79	1.2±0.1	1.3±0.2	179.3	120±25	60±8
20.68	2.0±0.1	2.1±0.2	193.1	164.24	66±8
27.58	2.9±0.1	3.0±0.2	206.8	220±20	71±8
34.47	3.9±0.1	4.0±0.2	220.6	290±15	77±9
41.37	4.8±0.1	5.0±0.3	234.4	376±19	82±10
48.26	5.9±0.1	6.0±0.3	248.2	482±41	88±11
55.16	7.0±0.1	7.1±0.3	262.0	609±80	94±12
62.05	8.1±0.1	8.3±0.4	275.8	762±133	99±14
68.95	9.2±0.1	9.4±0.4	289.6	945±205	105±16

^aPressure (MPa) equivalent to pressure (psi) 2K to 10K step 1K.

^bPressure (MPa) equivalent to pressure (psi) 26K to 42K step 2K.

Table 3. Composition B4, linear burning rate calculation

Pre-transition region			After-transition region		
Pressure ^a MPa	Burning rate, cm/s		Pressure ^b MPa	Burning rate, cm/s	
	Solid	Perf		Solid	Perf
13.79	0.5±0.2	0.8±0.3	179.3	689±33	296±45
20.68	1.4±0.2	1.8±0.2	193.1	765±34	296±37
27.58	3.0±0.3	3.2±0.1	206.8	843±35	296±31
34.47	5.5±1.0	4.9±1.7	220.6	924±38	296±24
41.37	9.1±2.6	7.1±3.3	234.4	1007±40	296±20
48.26	14.0±5.2	9.8±3.3	248.2	1092±43	296±16
55.16	20.3±8.9	13.0±5.2	262.0	1179±47	296±14
62.05	28.3±14.3	16.8±7.9	275.8	1268±52	297±14
68.95	38.2±21.4	21.1±11.1	289.6	1359±58	297±17

^aPressure (MPa) equivalent to pressure (psi) 2K to 10K step 1K.

^bPressure (MPa) equivalent to pressure (psi) 26K to 42K step 2K.

Table 4. Closed bomb burning rate of RDX - various particle sizes

<u>Pressure (MPa)</u>	<u>Burning rate, cm/s</u>			
	<u>605 (μ)</u>	<u>427 (μ)</u>	<u>301 (μ)</u>	<u>137 (μ)</u>
12	6.2	7.5	7.6	6.1
16	7.9	9.1	9.4	7.6
20	9.7	10.5	11.1	9.1
24	11.3	11.8	12.7	10.5
28	13.0	13.0	14.3	11.9
32	14.6	14.2	15.8	13.2
36	16.2	15.3	17.3	14.5
40	17.8	16.4	18.7	15.7

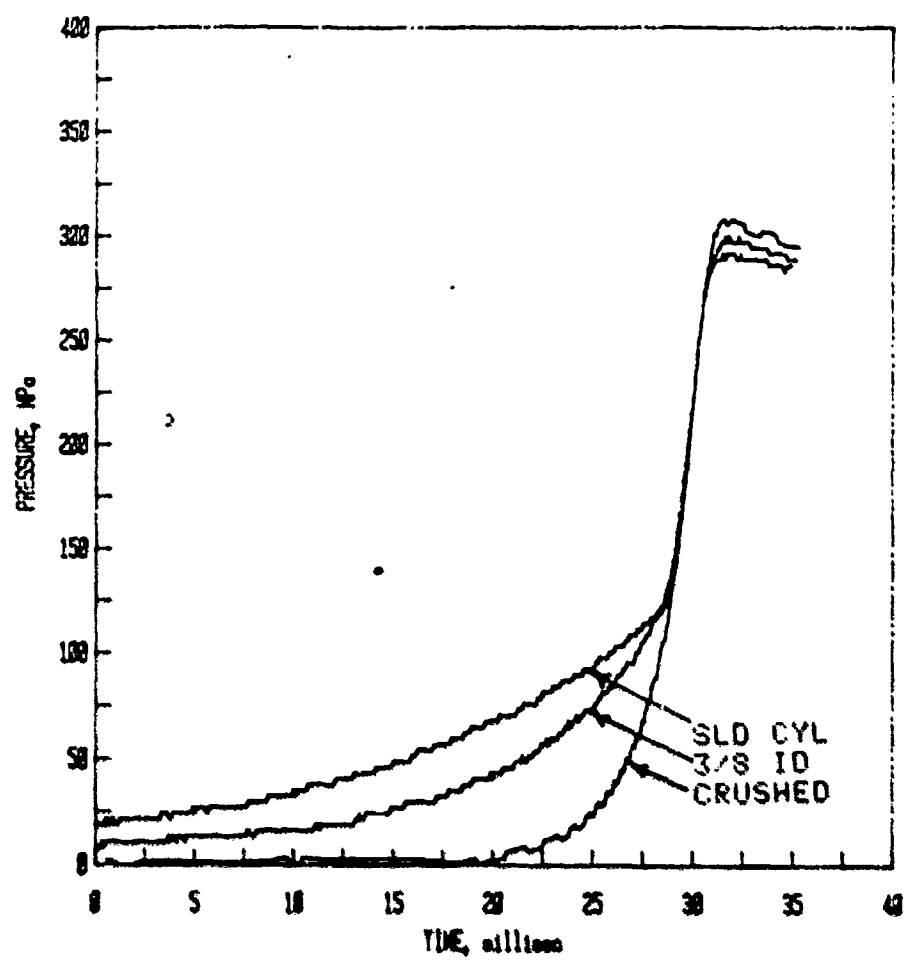


Figure 1. Comp B, solid cylinder, 3/8 single perf, and crushed

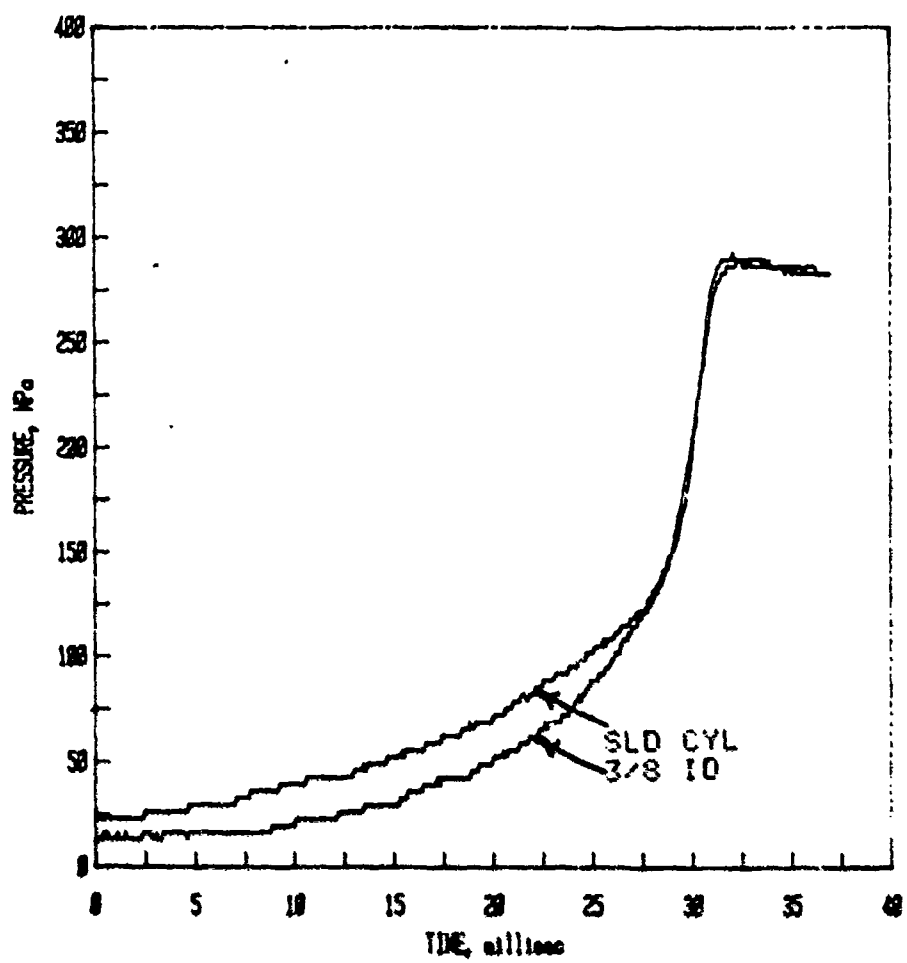


Figure 2. Composition BW, solid cylinder and 3/8" single perf (estane on RDX)

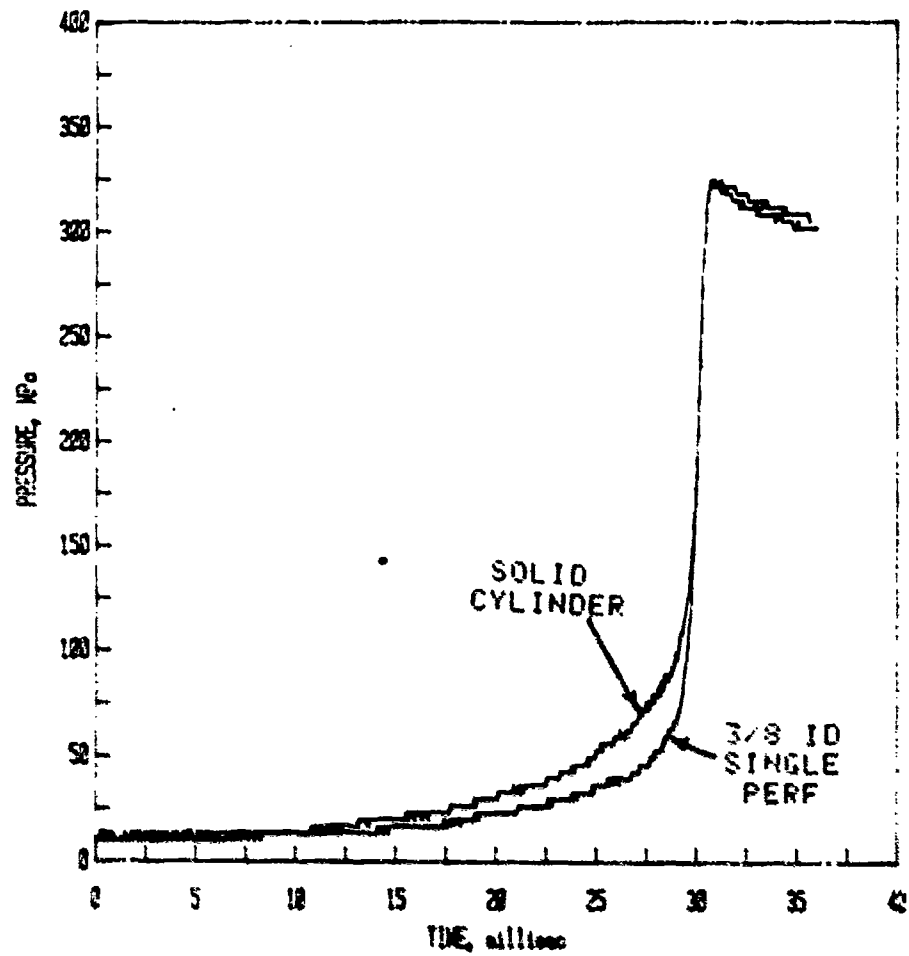


Figure 3. Composition 34, solid cylinder and single perf (without additives)

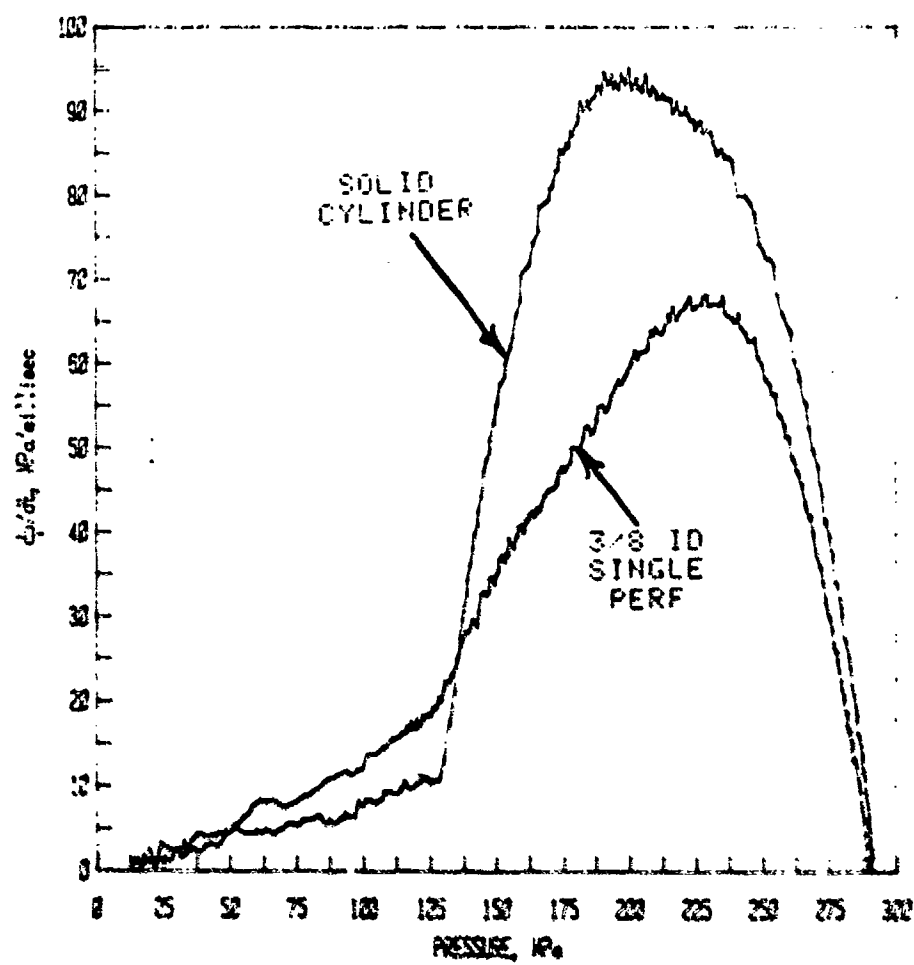


Figure 4. Composition B, standard type with wax, test #1

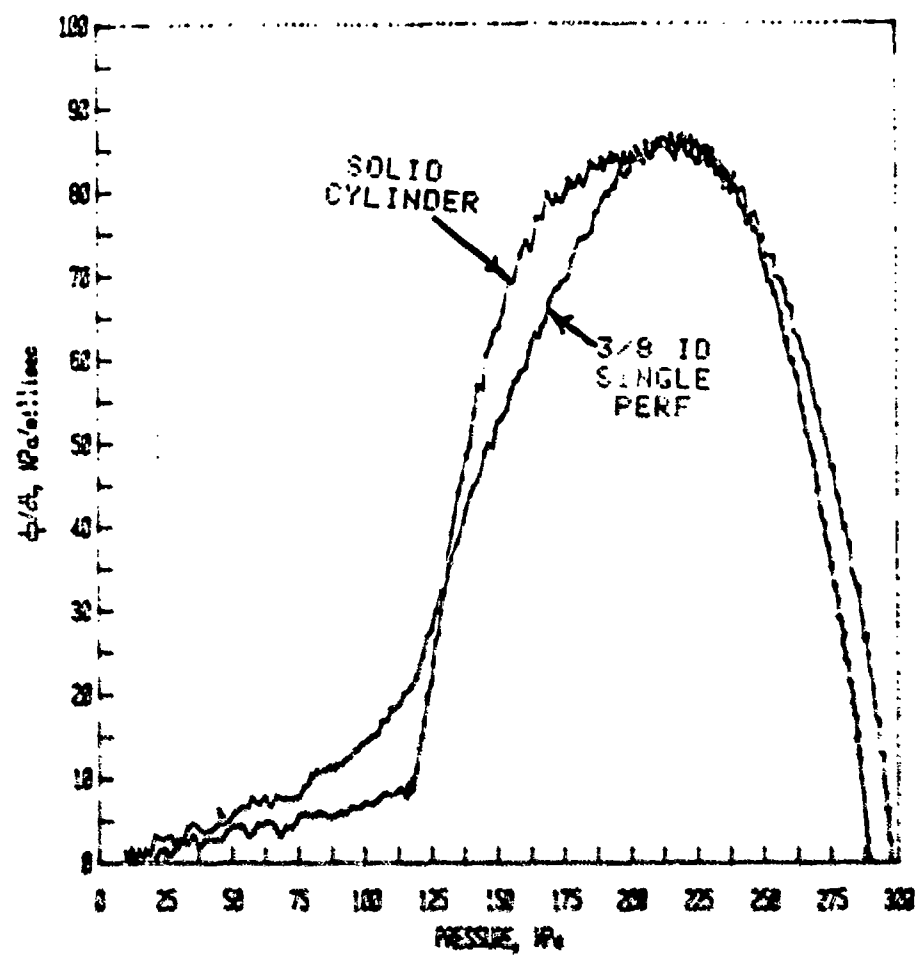


Figure 5. Composition B, standard type with wax, test #2

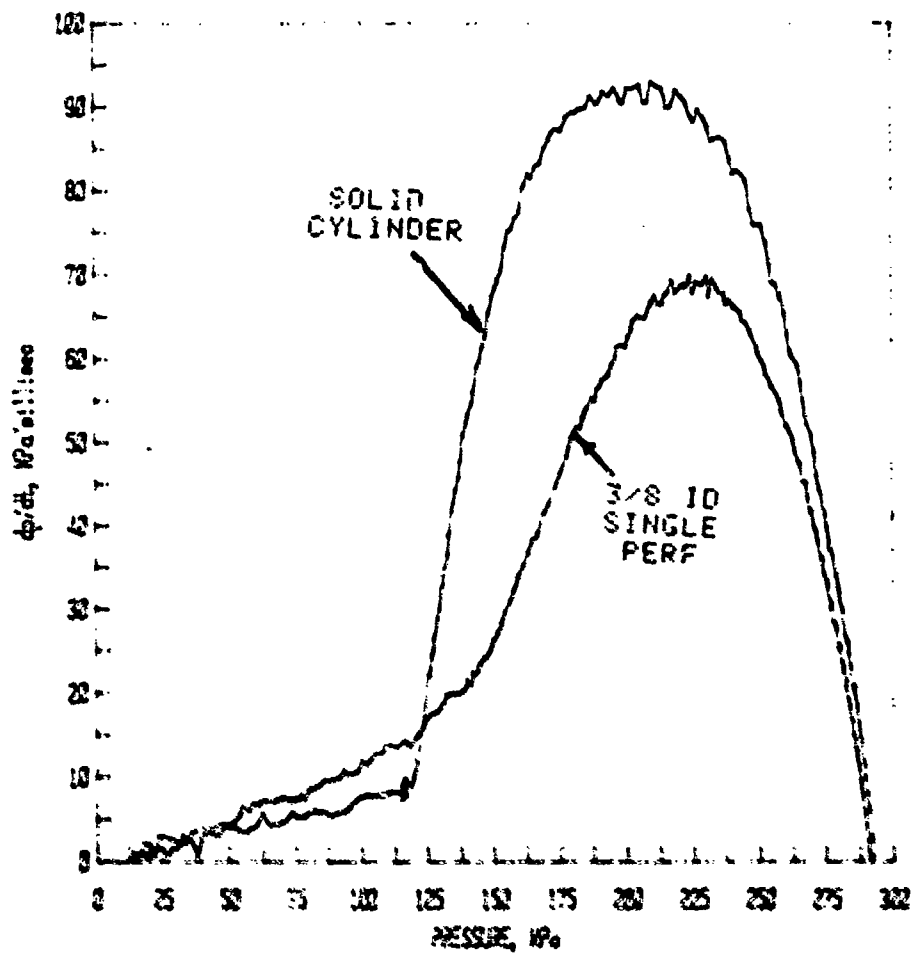


Figure 6. Composition B, standard type with wax, test #3

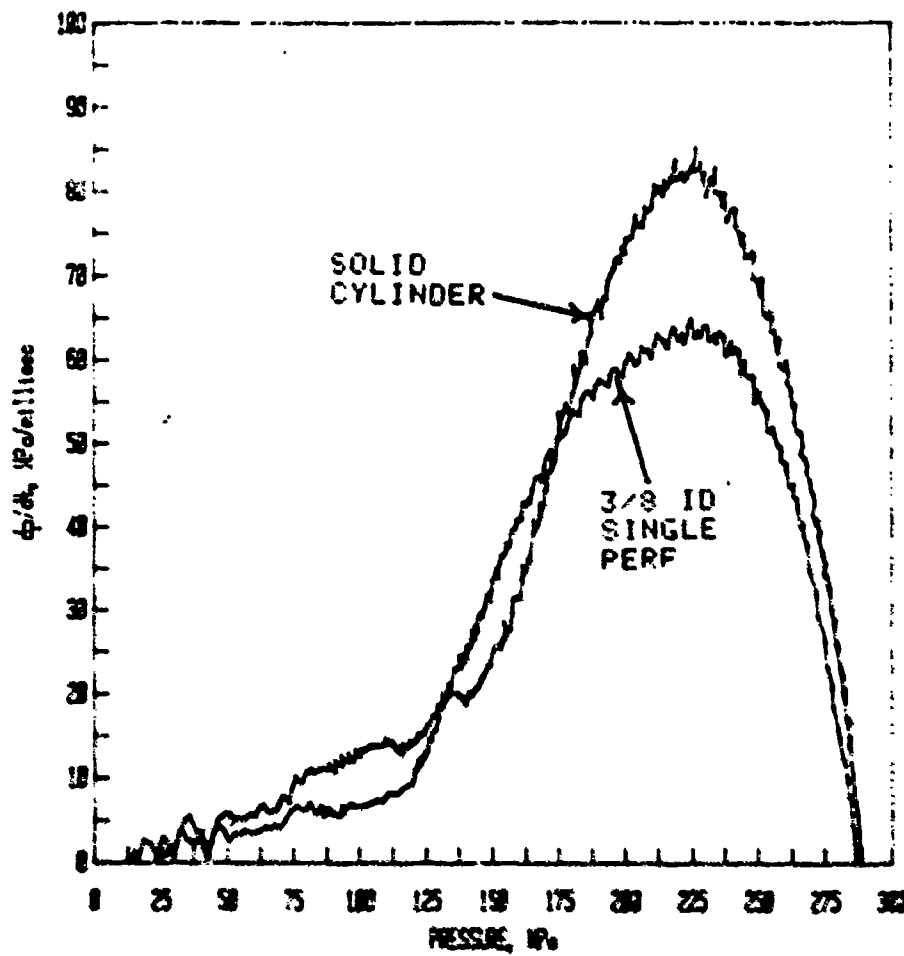


Figure 7. Composition BW, estane precoated on the RDX particle

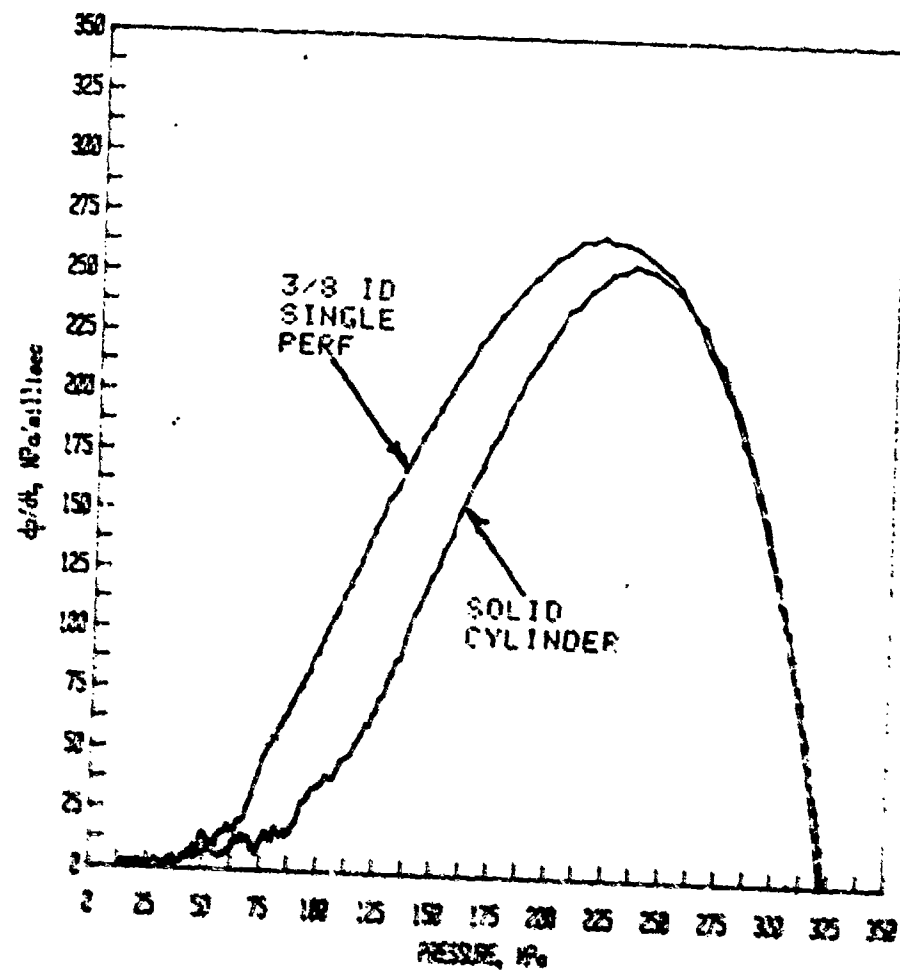


Figure 8. Composition B4, without additives

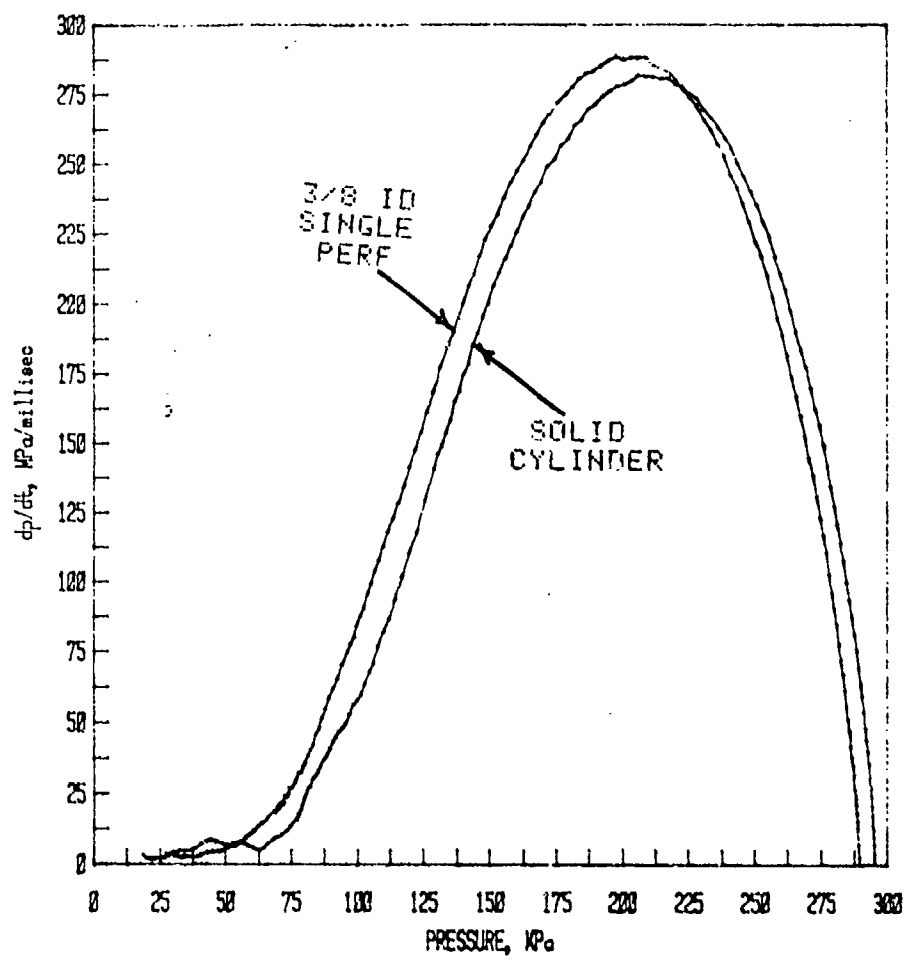


Figure 9. Composition A3, pressed to a density of 1.640 g/cm^3

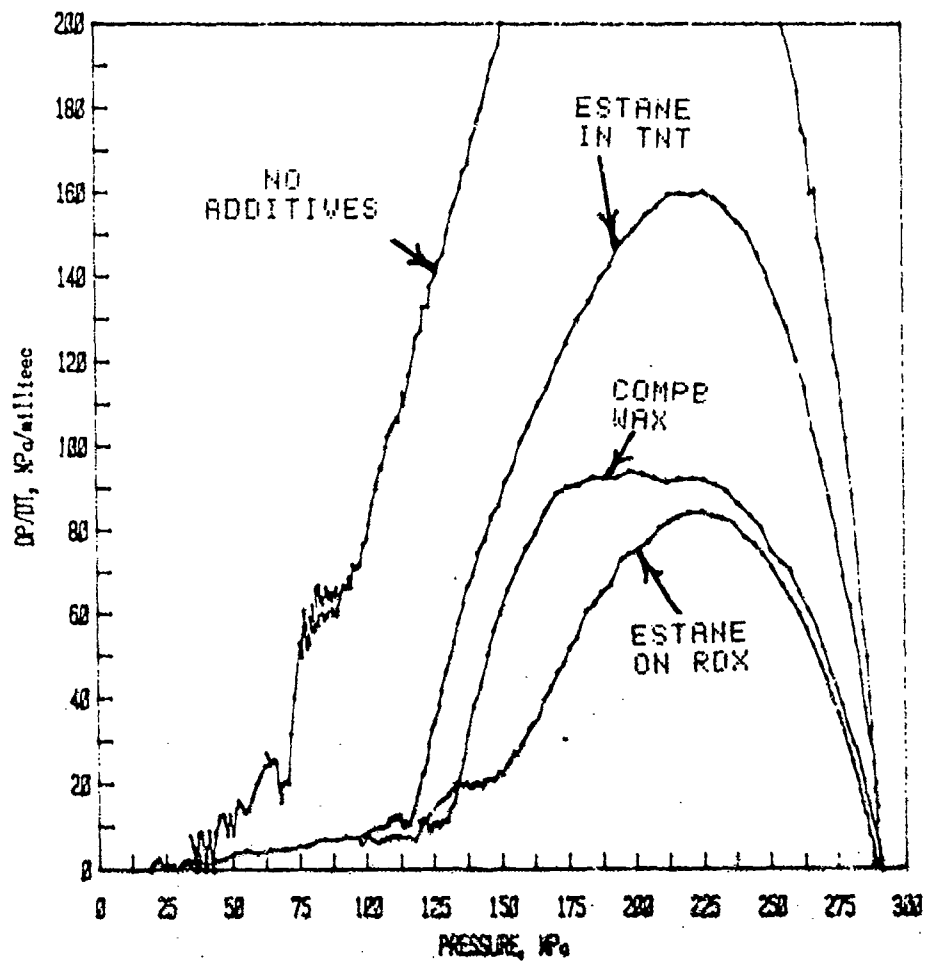


Figure 10. Comparison of additives in variations of Composition 8

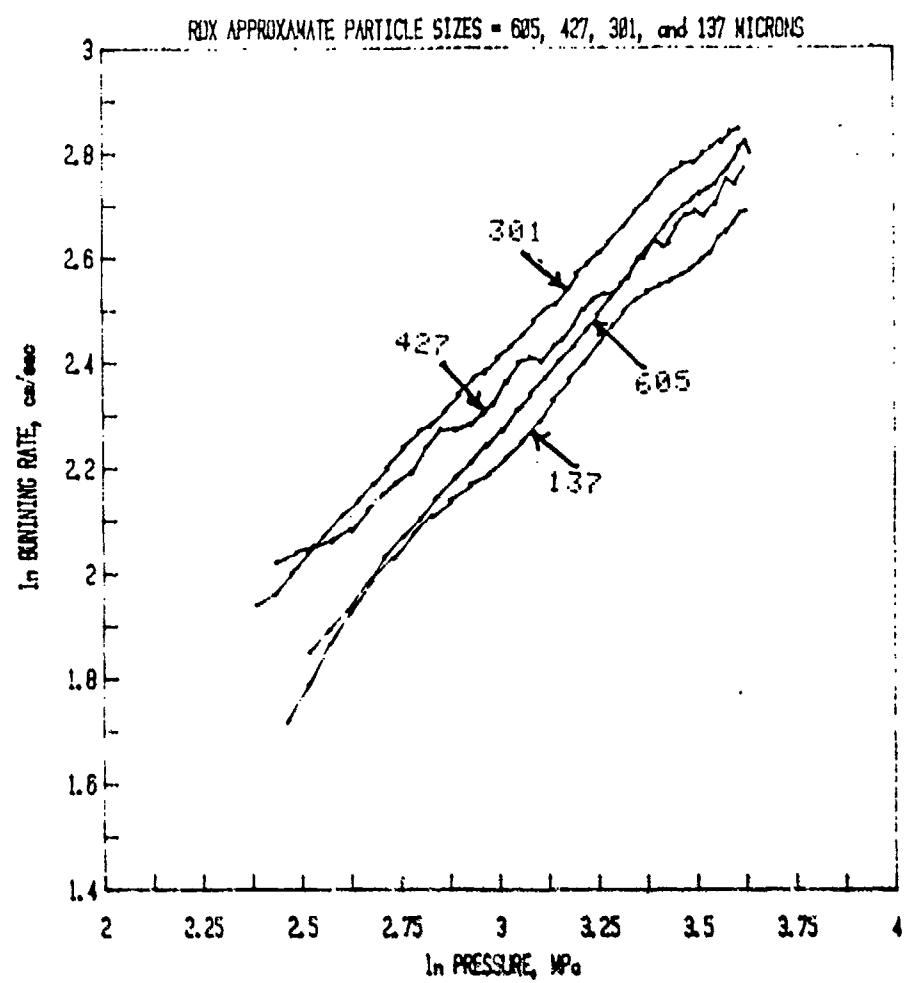


Figure 11. Closed bomb burning rates of the RDX particle

DISTRIBUTION LIST

Commander
U.S. Army Armament Research and
Development Command

ATTN: DRDAR-CG
DRDAR-LC
DRDAR-LCA, J. Lannon
D.S. Downs
A. Beardell
T. Vladimiroff
A. Grabowski
DRDAR-LCE, R.F. Walker (3)
DRDAR-LCE-D, R.W. Velicky (20)
DRDAR-LCM, L. Saffian
DRDAR-LCU, A. Moss
E.J. Zimpo
DRDAR-TDS, V. Lindner
DRDAR-TDC, D. Gyorg
DRDAR-GCL
DRDAR-TSS (5)

Dover, NJ 07801

Administrator
Defense Technical Information Center
ATTN: Accessions Division (12)
Cameron Station
Alexandria, VA 22314

Director
U.S. Army Materiel Systems
Analysis Activity
ATTN: DRXSY-MP
Aberdeen Proving Ground, MD 21005

Commander/Director
Chemical Systems Laboratory
U.S. Army Armament Research and
Development Command
ATTN: DRDAR-CLJ-L
DRDAR-CLB-PA
APG, Edgewood Area, MD 21010

Chief
Benet Weapons Laboratory, LCWSL
U.S. Army Armament Research and
Development Command
ATTN: DRDAR-LCB-TL
Watervliet, NY 12189

Director
Ballistics Research Laboratory
U.S. Army Armament Research and
Development Command
ATTN: DRDAR-TSB-S
DRDAR-BL, R.J. Eichelberger
DRDAR-BLT, P. Howe
R. Fifer
T. Cole
DRDAR-BLI, D. Anderson
D. Kooker
DRDAR-IB, E. Freedman
N. Gerri
H. Reeves
A. Juhasz
DRDAR-TB, R. Vitali
J.J. Trimble
R. Frey
I. May

Aberdeen Proving Ground, MD 21005

Commander
U.S. Army Armament Materiel
Readiness Command
ATTN: DRSAR-LEP-L
DRSAR-LEP-LM, R. Freeman
Rock Island, IL 61299

Director
U.S. Army TRADOC Systems
Analysis Activity
ATTN: ATAA-SL
White Sands Missile Range, NM 88002

Director
Industrial Base Engineering Activity
ATTN: DRXIB-MT
Rock Island, IL 61299

Office of Director of Defense
Research and Engineering
ATTN: K. Thorkildsen
Washington, DC 20314

Director
Advanced Research Projects Agency
Department of Defense
Washington, DC 20301

Headquarters
Department of the Army
Office of Deputy Chief of Staff for
Research Development and Acquisition
Munitions Division
ATTN: DAM-CSM-CA
Washington, DC 20310

Commander
U.S. Army Materiel Development and
Readiness Command
ATTN: DRCDMD-ST (2)
DRCSF-E, Mr. Mc Corkle (2)
5001 Eisenhower Avenue
Alexandria, VA 22333

Director
U.S. Army Systems Analysis Agency
ATTN: J. McCarthy
Aberdeen Proving Ground, MD 21005

Director
DARCOM Field Safety Activity
ATTN: DRXOS-ES
Charlestown, IN 47111

Commander
Harry Diamond Laboratories
ATTN: Technical Library
Branch 420, R.K. Warner
2800 Powder Mill Road
Adelphi, Md 20783

Commander
U.S. Army Research Office
ATTN: H. Robl
Box CM, Duke Station
Durham, NC 27706

Commander
Naval Ordnance Station
ATTN: W. Vreatt, Safety Dept.
M.C. Hudson
Code 5251B, S. Mitchell
Technology Ctr, Code 5037,
P. Fields
Technical Library
Indian Head, MD 20640

Commander
Naval Weapons Support Center
ATTN: Code 3031, D. Ellison
Crane, IN 47522

Commander
U.S. Naval Sea Systems Command
ATTN: E.A. Daugherty
SEA-064E, R.L. Beauregard
SEA-62YC (2)
SEA-62Y13C
Washington, DC 20362

Commander
U.S. Naval Weapons Center
ATTN: A. Amster
T.B. Joyner
Code 45, C.D. Lind
Code 388, T.L. Boggs
C.F. Price
A.I. Atwood
D.E. Zurn
R.L. Derr
Technical Library
Code 3273, Mr. Weathersby
China Lake, CA 93555

Commander
Naval Air Systems Command
ATTN: . AIR-310C, H. Rosenwasser
AIR-52321A, W. Zuke
Washington, DC 20361

Commander
Naval Weapons Station
ATTN: W. McBride
L.R. Rotherstein
Yorktown, VA 23491

Commander
Naval Coastal Systems Laboratory
Code 721, E. Richards
Code 722, J. Hammond
J. Kirkland
Code 741, D.W. Shepherd
Panama City, FL 32401

Commander
Naval Surface Weapons Center
ATTN: R12, S. Nesbitt
C. Laib
A. Compolattaro
D. Price
Technical Library
Silver Spring, MD 20910

Assistant General Manager for
Military Applications
U.S. Atomic Energy Commission
Washington, DC 20543

Commander
Air Force Armament Development and
Test Center
ATTN: AFB Technical Library
ADTC/DLIW, L. Elkins
DLDE, T.G. Floyd
G. Moy
Eglin Air Force Base, FL 32542

Director
U.S. Army Aeronautical Laboratory
Moffett Field, CA 94035

Bureau of Mines
4800 Forbes Avenue
ATTN: R.W. Watson
Pittsburgh, PA 15213

Director
NASA Ames Research Center
ATTN: Technical Library
Moffett Field, CA 94035

Director
Sandia Laboratories
ATTN: D. Anderson
R.J. Lawrence
J. Kennedy
D. Hayes
Technical Library
Albuquerque, NM 87115

Lawrence Livermore Laboratory
P.O. Box 808
ATTN: Technical Library
L402, R. McGuire
J.W. Kury
H.E. Rizzo
M. Flager
D. Orrnellas
L. Green
E. Lee
Livermore, CA 94550

McDonnel Aircraft Company
Department 353, Bldg. 33
ATTN: M.L. Schimmel
St. Louis, MO 63166

Los Alamos Scientific Laboratory

ATTN: Technical Library

WX-2, R.N. Rogers

G. Seay

X-4, MS250, C.A. Forest

B. Craig

R. Rabie

Los Alamos, NM 87544

Joseph Hershkowitz

305 Passaic Avenue

West Caldwell, NJ 07006

Bureau of Explosives

Association of American Railroads

ATTN: W.S. Chang

Raritan Center, Bldg. 812

Edison, NJ 08817

Princeton Combustion Research

Laboratories, Inc.

ATTN: M. Summerfield

1041 U.S. Highway One, North

Princeton, NJ 08540

Defense Logistics Studies

Information Exchange (2)

U.S. Army Logistics Management

Center

Fort Lee, VA 23801